# Hidden multiscale organization and robustness of real multiplex networks

Gangmin Son [1], Meesoon Ha [2,*] and Hawoong Jeong [1,3]

[1]*Department of Physics, Korea Advanced Institute of Science and Technology, Daejeon 34141, Korea*
[2]*Department of Physics Education, Chosun University, Gwangju 61452, Korea*
[3]*Center of Complex Systems, Korea Advanced Institute of Science and Technology, Daejeon 34141, Korea*

(Received 6 July 2023; accepted 20 December 2023; published 2 February 2024)

Hidden geometry enables the investigation of complex networks at different scales. Extending this framework to multiplex networks, we uncover a different kind of mesoscopic organization in real multiplex systems, named *clan*, a group of nodes that preserve local geometric arrangements across layers. Furthermore, we reveal the intimate relationship between the unfolding of clan structure and mutual percolation against targeted attacks, leading to an ambivalent role of clans: making a system fragile yet less prone to complete shattering. Finally, we confirm the correlation between the multiscale nature of geometric organization and the overall robustness. Our findings expand the significance of hidden geometry in network function, while also highlighting potential pitfalls in evaluating and controlling catastrophic failure of multiplex systems.

DOI: 10.1103/PhysRevE.109.024301

## I. INTRODUCTION

Complex systems possess an intricate architecture that spans multiple scales. The network geometry paradigm paves the way for exploring the multiscale organization of complex networks [1–4]. In particular, the concept of hidden metric spaces with hyperbolic geometry gives natural explanations for the common properties of real networks, such as degree heterogeneity, strong clustering, and small-world-ness [5–7]. Coarse graining of nodes based on their distances in a hidden metric space enriches the multiscale unfolding of networks [2,3]. For example, it allows studying self-similarity of the human connectome [8]. However, the study of multiscale organizations has still been limited to single-layer networks.

Indeed, many real networked systems consist of multiple interdependent systems represented by multilayer or multiplex networks, which are of theoretical and practical significance due to intriguing phenomena not seen in single-layer networks [9,10]. In multiplexes, if a node in one layer is attacked, its dependent nodes in the other layers break down as well. This interdependent nature can yield a catastrophic cascade of failures in mutual connectivity, which makes understanding the robustness of multiplex systems fascinating [11–22]. In this context, recent publications have demonstrated the significance of hidden geometry [23,24]: in real multiplexes, geometric organization correlated across layers, which can enhance their robustness against targeted attacks. Nonetheless, previous studies have only focused on the lack of interlayer independence based on mutual information [25]. Therefore, essential questions remain: How are the layers correlated across a range of scales? How do the multiscale properties affect the robustness?

In this paper, we show that the geometric correlations (GCs) of real multiplexes manifest across multiple scales rather than at a macroscopic scale. Notably, in contrast to the existing multiplex model for GCs [23,24], real multiplexes exhibit the decrease of GCs as coarse graining. Our model with the mesoscopic groups of mutually close nodes, named *clans* [26], accounts for such nontrivial behaviors. Moreover, clan structure drastically affects the robustness against targeted attacks in an ambivalent way: the macroscopic organization between clans makes a system fragile, whereas the mesoscopic organization within clans constrains complete shattering at the end. These phenomena are elucidated based on the conceptual analogy between clan unfolding and mutual percolation in both real systems and our model. Finally, we confirm that the GC spectra predict the robustness stemming from intra-clan organization among diverse real multiplex systems.

## II. MULTISCALE UNFOLDING OF MULTIFLEX NETWORKS

We start by extending the zooming-out technique of single-layer networks [2] to multiplexes (see Fig. 1). The approach relies on the assumption that each node in a network has radial and angular coordinates, $r_i$ and $\theta_i$, in a two-dimensional hyperbolic space [6]. Since the radial coordinate $r_i$ reflects the expected degree of the node, $\kappa_i$, we only focus on angular coordinates $\{\theta_i\}$. Given a network with the angular coordinates of nodes and a block size $\lambda$, consecutive $\lambda$ nodes along the circle are grouped into a supernode whose angular coordinate $\phi$ is defined by

$$\xi e^{\phi} = \frac{1}{\lambda}\sum_{j=1}^{\lambda} e^{i\theta_j}, \tag{1}$$

where $\theta_j$ is the angular coordinate of node $j$, and $\xi$ is the absolute value of the right-hand side [27]. Extending this to multiplexes, the same mapping should be applied to every layer. Therefore, one chooses a standard layer to define a mapping. The iteration of this process yields a sequence of downscaled versions per multiplex (see Fig. 1).

*Corresponding author: msha@chosun.ac.kr

 

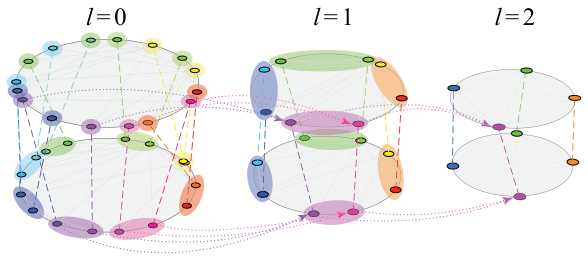


FIG. 1. Multiscale unfolding of multiplex networks. The downscaled versions of a duplex are schematically illustrated as the zooming-out level $l$ increases, $l = 0, 1, 2$ (from left to right). Each node has two angular coordinates for the upper and lower layers (gray disks). The colors of the nodes represent their angular coordinates in the lower layer, and dashed lines correspond to interlayer dependency links.

Measuring the GC [23,24] of downscaled versions yields a GC spectrum. For the sake of specificity, GCs were measured by the normalized mutual information (NMI) [25] between two sequences of angular coordinates in different layers; thus, we present the GC spectrum by the NMI as a function of the zooming-out level $l$ (see Supplemental Material (SM), Sec. I [28]). Here we investigate the GC spectra of real multiplexes (see SM, Sec. II and Table S1 [28]). Our aim is to compare real multiplexes with the existing model for GCs, called the geometric multiplex model (GMM). In the GMM, node $i$ at $\theta_{1,i}$ in layer 1 is assigned to $\theta_{2,i} = \theta_{1,i} + \Delta\theta_i$ in layer 2, where $\Delta\theta_i$ is an independent random variable. Thus, the GC is constructed at a macroscopic scale. To our aim, for a given multiplex, we obtain the GMM-like null counterpart, where the NMI for $l = 0$ and the topologies of layers are the same, but dependency links are rearranged by independent local noise as in the GMM (see SM, Sec. III [28]).

Figure 2(a) shows GC spectra for the arXiv collaboration (arXiv, A48) and the Internet (Internet, I12) multiplexes as well as the null counterparts with similar NMI values for $l = 0$. Strikingly, we observe a significant discrepancy between the original and the null. In the null, GC spectra tend to increase monotonically, indicating that independent local noise is washed out as coarse graining. However, in the original, NMI values can decrease by zooming out. This kind of discrepancy is found in other real systems in our dataset (see SM, Table S1 [28]), which can be quantified by the maximum difference as

$$m = \max_l [\mathrm{NMI}_{\mathrm{null}}(l) - \mathrm{NMI}_{\mathrm{org}}(l)]. \tag{2}$$

## III. CLAN STRUCTURE

To explain such nontrivial GC spectra in real multiplexes, we propose a multiplex model, named the multiscale geometric multiplex model (MGMM). Note that the NMI only indicates the lack of independence between two random variables, without specifying any particular correlation form, unlike the linear correlation coefficient, for instance. Therefore, a locally correlated yet globally uncorrelated configuration can also result in a nonzero NMI value. We introduce the groups of nodes preserving their local arrangement across layers, named *clans*, to our model, the MGMM. Specifically, each group of consecutive $\Lambda$ nodes in layer 1 is defined as a clan; a node $i$ is assigned to an angular coordinate in layer 2, $\theta_{2,i} = \theta_{1,i} + \Delta\theta_{\mathrm{clan}}$, where $\Delta\theta_{\mathrm{clan}}$ is the same for nodes in the same clan. Finally, the angular arrangement within a clan is preserved, but between clans is totally randomized (see SM, Sec. III [28]).

Figure 2(b) schematically illustrates the MGMM and its GMM-like null counterpart with their downscaled versions, and in Fig. 2(c), the MGMM with $\Lambda = 2^2$ exhibits no macroscopic correlations but four nodes in a clan are close to each other across layers. Such local correlations lead to a nonzero NMI value at $l = 0$ in Fig. 2(a) (model, original). When each clan becomes a supernode at the zooming-out level $l = 2$, the totally random organization between clans makes the downscaled version have no GCs. However, the GMM-like counterpart constructs a trivial linear correlation at a macroscopic scale, which leads to a monotonic increase in its GC

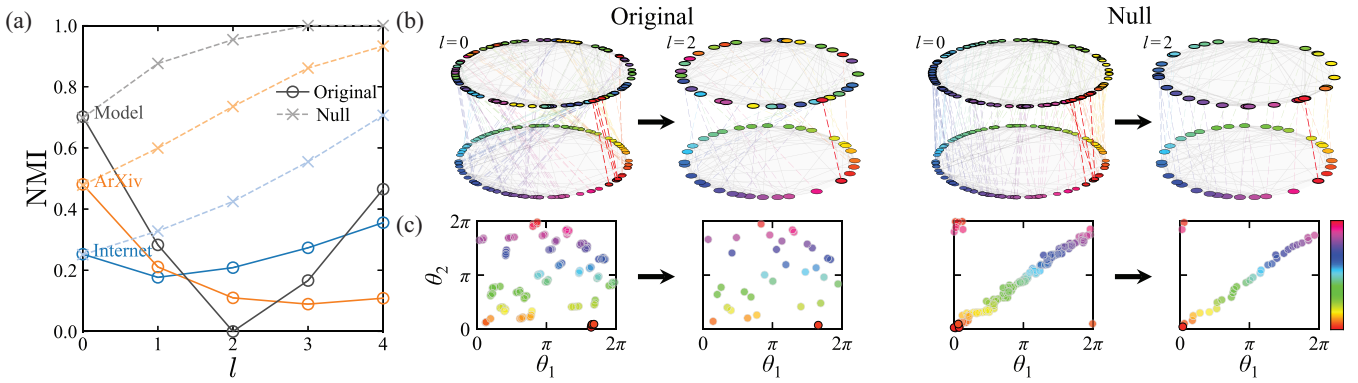


FIG. 2. Geometric correlation (GC) spectra of real multiplexes and multiscale geometric multiplex model (MGMM). (a) The normalized mutual information (NMI) [25] as a function of zooming-out level $l$ (with the coarse-graining block size $\lambda = 2$) for two sets of real data, i.e., arXiv (A48, orange circles) and Internet (I12, blue circles), and our model (MGMM, gray circles) with the total number of nodes, $N = 2^7$, in the comparison with their null counterparts (crosses with lighter colors). (b) Multiscale unfolding of a synthetic multiplex generated by the MGMM and its null counterpart. The upper (lower) layer represents $\theta_1$ ($\theta_2$). In the original, nodes in a planted clan are highlighted (red dashed lines) for $l = 0$ (left), which are coarse-grained into a single supernode for $l = 2$ (right). In the null, the corresponding nodes are also highlighted. (c) $(\theta_1, \theta_2)$ space. Highlighted clans are also marked as bold black edges. The color of each node corresponds to $\theta_2$ in (b) and (c).

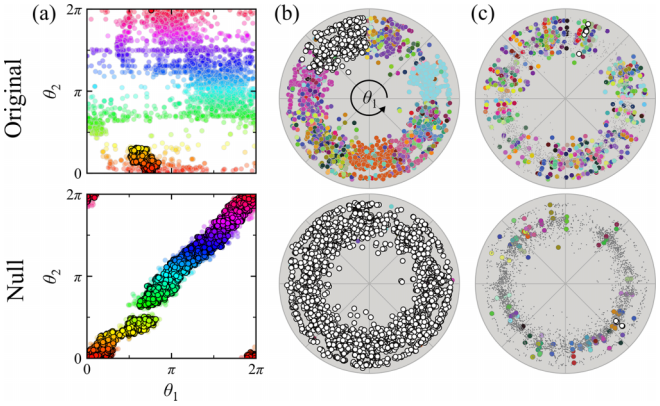


FIG. 3. Multiscale organization of Internet. (a) Angular coordinates of nodes in ($\theta_1$, $\theta_2$) space for the Internet (top) and its null counterpart (bottom). The color of each node corresponds to $\theta_2$. Identified clans in the original Internet (top) and its null counterpart (bottom) for (b) $z = 1/6$ ($\theta_w/\theta_c = 5$) and (c) $z = 2/3$ ($\theta_w/\theta_c = 0.5$). The presented maps are for layer 1. Clan memberships correspond to colors, and if the clan size is less than 3, nodes belonging to the clan are denoted as tiny gray dots. In particular, nodes in the largest clan are colored white and highlighted by bold black edges. Those in (b) are also highlighted in (a) in the same way.

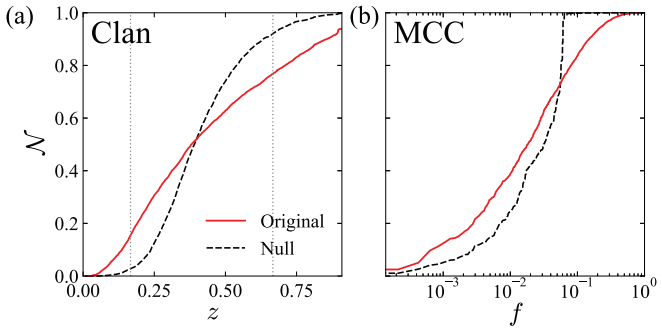


FIG. 4. Clan unfolding and mutual percolation in Internet. The rescaled number of clusters, $\mathcal{N}$, is plotted (a) for the clan against the resolution factor, $z$, and (b) for the mutually connected component (MCC) against the removal fraction of nodes, $f$, respectively. We compare the dynamics in the original multiplex (red solid lines) with its null counterpart (black dashed lines). The vertical gray dotted lines in (a) are drawn for $z = 1/6$ and $z = 2/3$ to indicate the instances in Fig. 3.

spectrum. Consequently, our model with clans accounts for the nontrivial behavior of the GC spectra, not present in the existing model. Then a question arises: Does clan structure appear in real multiplexes?

To answer the question, here we identify clans for a given multiplex. If the angular distance $d_{ij}$ between two nodes $i$ and $j$ is less than a certain angular window $\theta_w$, in both layers, they have the same clan membership. Concretely, a characteristic scale $\theta_c = 2\pi \ln N/N$ among $N$ points randomly distributed on a unit circle [29] allows us to define a resolution factor $z$ as

$$z = \frac{1}{1 + \theta_w/\theta_c}. \tag{3}$$

For $\theta_w = \infty$, $z = 0$ and all the nodes belong to a single clan, and for $\theta_w = 0$, $z = 1$ and all the clans correspond to isolated nodes. Figure 3 shows the identified clan structure of the Internet and its null counterpart. Although two multiplexes have the same GC at $l = 0$ [see Fig. 2(a)], the joint angular arrangements are clearly distinct from each other [Fig. 3(a)]. As in the comparison of the MGMM with the GMM [see Fig. 2(c)], in real multiplexes, layers seem uncorrelated at a macroscopic scale, while its null counterpart exhibits a clear linear correlation. This difference is reflected in the clan structure [Figs. 3(b) and 3(c)]. For $z = 1/6$, in the original, plenty of mesoscopic clans appear, whereas, in the null, most nodes belong to a giant clan. For $z = 2/3$, the null has more clans than the original, but most clans merely correspond to isolated nodes or pairs of nodes. Therefore, the nontrivial GC spectrum in Fig. 2(a) results in the appearance of mesoscopic clans in real multiplexes.

The qualitative discrepancy of clan structure in Fig. 3 becomes apparent by the number of clans, $\mathcal{N}_{\text{clan}}$, as a function of $z$ in Fig. 4(a). As expected in Fig. 3, a reversal occurs between $z = 1/6$ and $z = 2/3$, indicating that clan structure in the original leads to an earlier appearance of mesoscopic clans that remain longer as $z$ increases. Such results for various real multiplexes support the presence of the mesoscopic clan structure in real multiplexes (see SM, Sec. V and Figs. S3–S6 [28]).

## IV. ROLE OF CLANS IN ROBUSTNESS

By definition, clans are simply connected components in an overlapped proximity network, which allows us to identify the analogy between clan unfolding and mutual percolation in multiplexes [11,12]. First, the connection probability $p$ in the actual network is set as a function of the angular distance, $p \sim d^{1/T}$, where temperature $T$ controls the interaction range [6]. Although the power-law form implies long-range connections, the limitation of $T \to 0$ makes the connection probability similar to that in the proximity network. Second, mutual percolation concerns mutually connected components (MCCs), defined by a similar but less stringent constraint compared to the components derived from overlapped edges. Third, the targeted attack strategy, i.e., the removal of the highest-degree nodes, especially resembles the removal of the longest edges, i.e., the increase of $z$ in clan unfolding. Specifically, the expected value of the average angular length of edges incident to a node with the expected degree $\kappa$ is given by

$$\int d(\theta, \theta')p(\theta, \kappa, \theta', \kappa')\mathrm{d}\theta\mathrm{d}\theta'\mathrm{d}\kappa' \sim \ln \kappa. \tag{4}$$

As a result, we conjecture that clan structure also plays an analogous role in mutual percolation against targeted attacks. Since our analysis controls macroscopic GCs, this notion alludes to the origins of the robustness of real multiplexes beyond Ref. [24] (see SM, Table S2 [28] for the summary of the analogy).

Figure 4(b) shows the number of MCCs as a function of the removal fraction of nodes $f$ against targeted attacks. Remarkably, similarly to the results of clan unfolding in Fig. 4(a), the relative order of $\mathcal{N}_{\text{MCC}}$ between the original and the null is reversed. However, the analogy is not

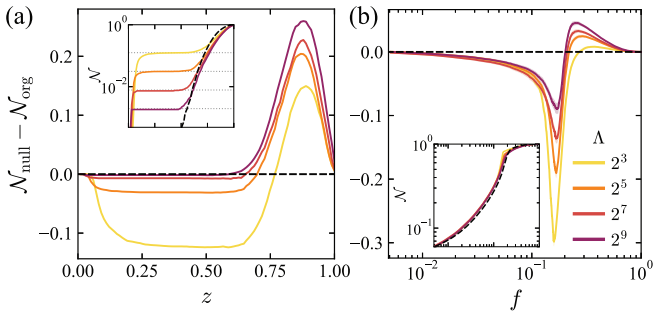


FIG. 5. Clan unfolding and mutual percolation in MGMM. Synthetic multiplexes are generated by the MGMM [30] for the total number of nodes, $N = 2^{12}$, and the planted clan size $\Lambda \in \{2^3, 2^5, 2^7, 2^9\}$. The difference of $\mathcal{N}$ between the null (black dashed line) and the original instances (solid lines) are plotted (a) for the clan against $z$ and (b) for the MCC against $f$. Insets show the raw values of $\mathcal{N}$, and the horizontal gray dotted lines in the inset of (a) represent $1/\Lambda$ for each $\Lambda$.

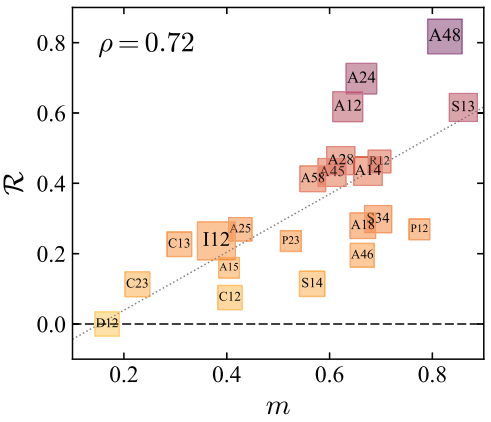


FIG. 6. Correlation between $\mathcal{R}$ and $m$ for 22 real multiplexes (see SM, Table S1 [28] for detailed information). The black dashed line indicates $\mathcal{R} = 0$. The gray dotted line guides linear regression results. Square sizes correspond to the logarithm of system sizes, and colors to $\mathcal{R}$ for visual convenience.

complete, so the apparent reversal in mutual percolation is not common in real multiplexes. However, they tend to have the smaller $\mathcal{N}_{\rm MCC}$, implying that clan structure impedes complete breakdown against targeted attacks (see SM, Sec. V and Figs. S7–S10 [28]).

In order to systematically investigate the role of clans in mutual percolation, we employ synthetic networks generated by the MGMM for a variety of the planted clan size $\Lambda$. In Figs. 5(a) and 5(b), we present $\mathcal{N}$ for clan unfolding and mutual percolation in synthetic networks, respectively. Given that GCs are similar to high NMI values (NMI $\approx 0.9$) as $\Lambda$ varies, we take a single null counterpart for them. Notably, the crossing behaviors of the number of clans as $\Lambda$ varies [Fig. 5(a)] are reflected in those of MCCs [Fig. 5(b)], which demonstrates the ambivalent role of clans in percolation dynamics. In the MGMM, as $\Lambda$ increases, the size of planted clans grows and their number decreases, exposed as the plateaus in the inset of Fig. 5(a), so the intra-clan organization becomes dominant over the inter-clan. Therefore, we find that for larger $\Lambda$, the crossing becomes less pronounced, but the final-stage robustness increases. Although the incompleteness of the analogy blurs the plateaus, the planted clan size $\Lambda$ plays a qualitatively similar role in both clan unfolding and mutual percolation (see SM, Sec. V and Fig. S11 [28]).

Finally, from the implications of model results, we examine correlations between the nontrivial multiscale nature of geometric organization and robustness stemming from intra-clan organization in real systems. The multiscale nature of a multiplex can be quantified by the discrepancy in the GC spectrum with its null counterpart $m$ defined in Eq. (2). The inter-clan robustness $\mathcal{R}$ can be defined by the suppression of complete shattering at the final stage observed in Figs. 4(b) and 5(b), as follows:

$$\mathcal{R} = \max_f [\mathcal{N}_{\rm null} - \mathcal{N}_{\rm org}]. \tag{5}$$

In other words, $\mathcal{R}$ describes how mesoscopic MCCs remaining after the removal of hubs are durable. In Fig. 6, we find a strong positive correlation between the multiscale nature in GCs, $m$, and the robustness $\mathcal{R}$, (Pearson correlation coefficient $\rho \approx 0.72$ with the p-value $\approx 0.0002$). This supports our conjecture based on model results and emphasizes the significance of multiscale organization in percolation dynamics of real multiplexes.

## V. CONCLUSION

To sum up, we filled the crucial gap between the existing multiplex model for geometric correlations (GCs) [23,24] and real multiplexes by hidden multiscale groups of mutually close nodes, i.e., *clans*. Remarkably, clans dictate the breakdown of mutual connectivity against targeted attacks, solely related to network topology, which highlights the power of the network geometry paradigm in elucidating network function through low-dimensional geometric patterns [31]. This also implies that if clan structure is ignored in a multiplex, its robustness could be both over- and underestimated. Thus, the investigation of multiscale organizations has many applications to real systems [32], from the brain and power grids to physical materials [33]. The role of multiscale organizations on cascading failures [22] is also a promising topic.

## ACKNOWLEDGMENTS

We would like to thank M. Á. Serrano for helpful comments on the manuscript. This research was supported by the Basic Science Research Program through the National Research Foundation of Korea (NRF) (KR) [Grants No. NRF-2020R1A2C1007703 (G.S., M.H.) and No. NRF-2022R1A2B5B02001752 (G.S., H.J.)].

[1] M. Boguñá, I. Bonamassa, M. De Domenico, S. Havlin, D. Krioukov, and M. Á. Serrano, Network geometry, Nat. Rev. Phys. **3**, 114 (2021).

[2] G. García-Pérez, M. Boguñá, and M. Á. Serrano, Multiscale unfolding of real networks by geometric renormalization, Nat. Phys. **14**, 583 (2018).

[3] M. Zheng, G. García-Pérez, M. Boguñá, and M. Á. Serrano, Scaling up real networks by geometric branching growth, Proc. Natl. Acad. Sci. **118**, e2018994118 (2021).

[4] P. Villegas, T. Gili, G. Caldarelli, and A. Gabrielli, Laplacian renormalization group for heterogeneous networks, Nat. Phys. **19**, 445 (2023).

[5] M. Á. Serrano, D. Krioukov, and M. Boguñá, Self-similarity of complex networks and hidden metric spaces, Phys. Rev. Lett. **100**, 078701 (2008).

[6] D. Krioukov, F. Papadopoulos, M. Kitsak, A. Vahdat, and M. Boguñá, Hyperbolic geometry of complex networks, Phys. Rev. E **82**, 036106 (2010).

[7] F. Papadopoulos, M. Kitsak, M. Á. Serrano, M. Boguñá, and D. Krioukov, Popularity versus similarity in growing networks, Nature (London) **489**, 537 (2012).

[8] M. Zheng, A. Allard, P. Hagmann, Y. Alemán-Gómez, and M. Á. Serrano, Geometric renormalization unravels self-similarity of the multiscale human connectome, Proc. Natl. Acad. Sci. **117**, 20244 (2020).

[9] S. Boccaletti, G. Bianconi, R. Criado, C. I. del Genio, J. Gómez-Gardeñes, M. Romance, I. Sendiña-Nadal, Z. Wang, and M. Zanin, The structure and dynamics of multilayer networks, Phys. Rep. **544**, 1 (2014).

[10] G. Bianconi, *Multilayer Networks*, Vol. 1 (Oxford University Press, Oxford, 2018).

[11] S. V. Buldyrev, R. Parshani, G. Paul, H. E. Stanley, and S. Havlin, Catastrophic cascade of failures in interdependent networks, Nature (London) **464**, 1025 (2010).

[12] S.-W. Son, G. Bizhani, C. Christensen, P. Grassberger, and M. Paczuski, Percolation theory on interdependent networks based on epidemic spreading, Europhys. Lett. **97**, 16006 (2012).

[13] G. J. Baxter, S. N. Dorogovtsev, A. V. Goltsev, and J. F. F. Mendes, Avalanche collapse of interdependent networks, Phys. Rev. Lett. **109**, 248701 (2012).

[14] J. Gao, S. V. Buldyrev, S. Havlin, and H. E. Stanley, Robustness of a network of networks, Phys. Rev. Lett. **107**, 195701 (2011).

[15] G. Dong, J. Gao, R. Du, L. Tian, H. E. Stanley, and S. Havlin, Robustness of network of networks under targeted attack, Phys. Rev. E **87**, 052804 (2013).

[16] G. Bianconi, Dangerous liaisons? Nat. Phys. **10**, 712 (2014).

[17] G. J. Baxter, S. N. Dorogovtsev, J. F. F. Mendes, and D. Cellai, Weak percolation on multiplex networks, Phys. Rev. E **89**, 042801 (2014).

[18] S. D. Reis, Y. Hu, A. Babino, J. S. Andrade, Jr, S. Canals, M. Sigman, and H. A. Makse, Avoiding catastrophic failure in correlated networks of networks, Nat. Phys. **10**, 762 (2014).

[19] G. J. Baxter, G. Bianconi, R. A. da Costa, S. N. Dorogovtsev, and J. F. F. Mendes, Correlated edge overlaps in multiplex networks, Phys. Rev. E **94**, 012303 (2016).

[20] D. Cellai, E. López, J. Zhou, J. P. Gleeson, and G. Bianconi, Percolation in multiplex networks with overlap, Phys. Rev. E **88**, 052811 (2013).

[21] B. Min, S. D. Yi, K.-M. Lee, and K.-I. Goh, Network robustness of multiplex networks with interlayer degree correlations, Phys. Rev. E **89**, 042811 (2014).

[22] B. Gross, I. Bonamassa, and S. Havlin, Dynamics of cascades in spatial interdependent networks, Chaos **33**, 103116 (2023).

[23] K.-K. Kleineberg, M. Boguñá, M. Ángeles Serrano, and F. Papadopoulos, Hidden geometric correlations in real multiplex networks, Nat. Phys. **12**, 1076 (2016).

[24] K.-K. Kleineberg, L. Buzna, F. Papadopoulos, M. Boguñá, and M. Á. Serrano, Geometric correlations mitigate the extreme vulnerability of multiplex networks against targeted attacks, Phys. Rev. Lett. **118**, 218301 (2017).

[25] A. Kraskov, H. Stögbauer, and P. Grassberger, Estimating mutual information, Phys. Rev. E **69**, 066138 (2004).

[26] The term has been used in Ref. [34] as a group of nodes with similar angular coordinates in the single-layer context.

[27] A. Faqeeh, S. Osat, and F. Radicchi, Characterizing the analogy between hyperbolic embedding and community structure of complex networks, Phys. Rev. Lett. **121**, 098301 (2018).

[28] See Supplemental Material at http://link.aps.org/supplemental/10.1103/PhysRevE.109.024301 for more details, which includes Refs. [2,5,6,23–25,27,35–38].

[29] K. Zuev, M. Boguná, G. Bianconi, and D. Krioukov, Emergence of soft communities from geometric preferential attachment, Sci. Rep. **5**, 9421 (2015).

[30] Here, the other parameters of the MGMM are set for a power-law degree distribution with the degree exponent $\gamma = 2.6$, the average degree $\langle k \rangle \approx 8$, and temperature $T = 0.7$.

[31] J. van der Kolk, G. García-Pérez, N. E. Kouvaris, M. Á. Serrano, and M. Boguñá, Emergence of geometric turing patterns in complex networks, Phys. Rev. X **13**, 021038 (2023).

[32] M. De Domenico, More is different in real-world multilayer networks, Nat. Phys. **19**, 1247 (2023).

[33] I. Bonamassa, B. Gross, M. Laav, I. Volotsenko, A. Frydman, and S. Havlin, Interdependent superconducting networks, Nat. Phys. **19**, 1163 (2023).

[34] E. Ortiz and M. Á. Serrano, Multiscale voter model on real networks, Chaos Solitons Fractals **165**, 112847 (2022).

[35] A. M. Abdolhosseini-Qomi, S. H. Jafari, A. Taghizadeh, N. Yazdani, M. Asadpour, and M. Rahgozar, Link prediction in real-world multiplex networks via layer reconstruction method, R. Soc. Open Sci. **7**, 191928 (2020).

[36] F. Papadopoulos, R. Aldecoa, and D. Krioukov, Network geometry inference using common neighbors, Phys. Rev. E **92**, 022807 (2015).

[37] F. Papadopoulos, C. Psomas, and D. Krioukov, Network mapping by replaying hyperbolic growth, IEEE/ACM Trans. Network. **23**, 198 (2015).

[38] G. García-Pérez, A. Allard, M. Á. Serrano, and M. Boguñá, Mercator: Uncovering faithful hyperbolic embeddings of complex networks, New J. Phys. **21**, 123033 (2019).